

Synthesis, structure and physical properties of a new organic metal, (BEDO-TTF)₄[C₄N₆]²⁻·H₂O

Brian H. Ward,^a Garrett E. Granroth,^b James B. Walden,^b Khalil A. Abboud,^a Mark W. Meisel,^{*b} Paul G. Rasmussen^{*c} and Daniel R. Talham^{*a}

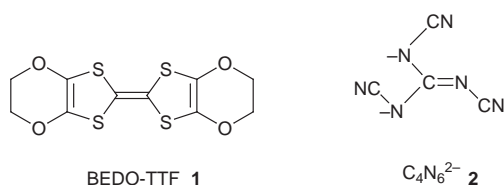
^aDepartment of Chemistry, University of Florida, PO Box 117200, Gainesville, Florida 32611-7200, USA

^bDepartment of Physics, University of Florida, PO Box 118440, Gainesville, Florida 32611-8440, USA

^cDepartment of Chemistry, Willard H. Dow Laboratories, The University of Michigan, Ann Arbor, Michigan 48109-1055, USA

A new organic metal based on the π -donor bis(ethylenedioxy)tetrathiafulvalene, (BEDO-TTF)₄[C₄N₆]²⁻·H₂O, has been isolated as the *N,N',N''*-tricyanoguanidinate monohydrate salt. The crystal structure indicates strong two-dimensional (2D) behavior in the BEDO-TTF donor layer demonstrated by the close intermolecular C—H...O, S...S, and S...O contacts. The *N,N',N''*-tricyanoguanidinate dianions are puckered and form dimers through hydrogen bonding with two water molecules, resulting in an infinite sheet of dianions that complement the 2D nature of the BEDO-TTF donor layers. Four-probe resistance, tunnel diode oscillator, and EPR measurements indicate metallic behavior down to 8 K where a metal–semiconductor transition occurs. (BEDO-TTF)₄[C₄N₆]²⁻·H₂O crystallizes in the $P\bar{1}$ space group with $a = 11.9628(2)$, $b = 14.1016(2)$, $c = 17.0830(2)$ Å, $\alpha = 81.27(1)$, $\beta = 70.21(1)$, $\gamma = 77.04(1)^\circ$, $V = 2633.39(7)$ Å³, $Z = 2$.

Since the discovery of superconductivity in tetramethyltetraselenafulvalene perchlorate, (TMTSF)₂ClO₄,¹ there has been interest in developing further examples of organic molecular conductors and superconductors. Cation-radical salts based on the donor bis(ethylenedithio)tetrathiafulvalene (BEDT-TTF) have been the most fruitful class of materials, from which over 50 superconductors are currently known.² Among the BEDT-TTF cation-radical salts, κ -(BEDT-TTF)₂Cu[N(CN)₂]Br has the highest ambient pressure superconducting transition temperature with $T_c = 11.6$ K.³ Many other organic donor molecules have been developed for the purpose of preparing molecular conductors.² One of the more interesting is bis(ethylenedioxy)tetrathiafulvalene, (BEDO-TTF) **1**, first prepared by Suzuki *et al.* in 1989.⁴ Substitution of sulfur by oxygen in the outer ring of BEDT-TTF lowers the oxidation potential and increases electron density on the TTF core, while keeping the size and shape of the molecule the same.⁵ There are now many BEDO-TTF based cation-radical salts including two superconductors.^{6–10} Interestingly, despite the similar size and shape of the donors, BEDO-TTF cation-radical salts form with different crystal packing motifs from those seen with BEDT-TTF.



Several of the known conducting BEDO-TTF salts form with organic acceptors or organic anions. Horiuchi recently reported crystal structures of several new BEDO-TTF cation-radical salts including four with cyano-rich organic anions.¹⁰ While the monoanion of cyanoform (C₄N₃⁻) forms a 5:2 salt, the monoanion 1,1,2,3,3-pentacyanopropenide (C₈N₅⁻) forms a 2:1, salt and both systems are conducting. BEDO-TTF forms 4:1 salts with the dianions hexacyanotrimethylene-

methanediide (C₁₀N₆²⁻, HCTMM) and tris(dicyanomethylene)cyclopropanediide (C₁₂N₆²⁻, HCP). Both of these 4:1 salts are also metallic.

The dianion *N,N',N''*-tricyanoguanidinate **2** was recently described by Subrayan *et al.* as part of studies into molecules containing only carbon and nitrogen.¹¹ The dianion **2** has alternating C—N connectivity with an open chain structure rather than the cyclic aromatic triazine structure common among high nitrogen compounds. Subrayan *et al.* describe a facile preparation of **2** which can be isolated as the sodium or potassium salt.¹¹ Considering the novel dianion to be potentially useful as a counterion for preparing cation-radical salts, we have used **2** in electrocrystallization cells with the donor BEDO-TTF. The title compound (BEDO-TTF)₄[C₄N₆]²⁻·H₂O **3** has been isolated and is a new example of a BEDO-TTF molecular conductor. (BEDO-TTF)₄[C₄N₆]²⁻·H₂O is metallic from room temperature down to 8 K, below which point the conductivity begins to decrease. Results of the synthesis, crystal structure, magnetic and transport properties, and how they compare to other BEDO-TTF salts are the subjects of this paper.

Experimental details

Materials

BEDO-TTF was synthesized according to the method described by Suzuki⁵ and recrystallized twice from cyclohexane. Disodium *N,N',N''*-tricyanoguanidinate (Na₂C₄N₆·H₂O) was prepared as previously described and recrystallized from an ethanol–water (4:1) mixture.¹¹ 1,4,7,10,13-Pentaoxacyclopentadecane or 15-crown-5 (C₁₀H₂₀O₅, 98%) was purchased from Aldrich Chemical Co. (Milwaukee, WI). Methylene chloride (CH₂Cl₂, 99.9%) and absolute ethanol (C₂H₅OH) were purchased from Fisher Scientific (Orlando, FL). Methylene chloride was dried over P₂O₅ and distilled before use, while ethanol and 15-crown-5 were used without further purification.

Synthesis of (BEDO-TTF)₄[C₄N₆]₄·H₂O **3**

BEDO-TTF (7.0 mg) was placed in the working arm of a two-electrode H-cell and dissolved in 30 ml of 9.75 mM disodium *N,N',N''*-tricyanoguanidinate in 15% EtOH–methylene chloride containing 20 drops of 15-crown-5. A constant current density of 0.70 μA cm⁻² was maintained at room temperature between the platinum working electrode and counter electrode that were separated by two glass frits. After a few days elongated plates of **3** could be seen on the electrode surface and at the bottom of the H-cell. Large (typically 2.5 × 1.0 × 0.5 mm³) black plates of **3** were collected after 21 d.

Crystallographic data collection and structure determination

Data for **3** were collected at 173 K on a Siemens SMART platform equipped with a charge-coupled device (CCD) area detector and a graphite monochromator utilizing Mo-Kα radiation (λ = 0.71073 Å). Cell parameters were refined using 8151 reflections. A hemisphere of data (1381 frames) was collected using the ω-scan method (0.3° frame width). The first 50 frames were remeasured at the end of data collection to monitor instrument and crystal stability (maximum correction on *I* was < 1%). ψ-scan absorption corrections were applied based on the entire data set.

The structure was solved by direct methods in SHELXTL⁵¹² and refined using full-matrix least-squares analysis. The asymmetric unit consists of four BEDO-TTF molecules, one tricyanoguanidinate dianion, and a disordered water molecule (site occupation factors are 0.49(4) and 0.51(4) for O1 and O1', respectively). The H atoms of the partial water molecules are not disordered. They were obtained from a difference Fourier map, and their coordinates were refined while their isotropic thermal parameters were calculated at 1.5 of that of the O atoms. One end of one of the BEDO-TTF molecules is disordered with one CH₂–CH₂ unit having a refined occupation factor of 0.59(2) and the other 0.41(2). All non-H atoms were treated anisotropically, whereas the hydrogen atoms were calculated in ideal positions and were riding on their respective carbon atoms. A total of 774 parameters were refined in the final cycle of refinement using 5824 reflections with *I* > 2σ(*I*) to yield *R*1 4.61% and *wR*2 of 10.12%, respectively. Refinement was done using *F*². Full crystallographic details, excluding structure factors, have been deposited at the Cambridge Crystallographic Data Centre (CCDC). See Information for Authors, *J. Mater. Chem.*, 1998, Issue 1. Any request to the CCDC for this material should quote the full literature citation and the reference number 1145/87.

EPR measurements

Electron paramagnetic resonance (EPR) spectra of **3** were recorded between 4 and 298 K using a Bruker (Billerica, MA) ER-200D spectrometer modified with a digital signal channel and a digital field controller. In addition the spectrometer was equipped with an Oxford Instruments (Witney, England) ITC 503 temperature controller and ESR 900 cryostat supplied with an AuFe/chromel thermocouple for temperature dependent studies. A (BEDO-TTF)₄[C₄N₆]₄·H₂O single crystal (1.5 × 1.0 × 0.05 mm³) was selected and mounted on a cut edge of a quartz rod; rotation was achieved using a home-built goniometer. The sample was first mounted vertically in the microwave cavity. The 0° and 90° orientations correspond to the perpendicular and parallel alignments, respectively, of the crystal *ab* plane with respect to the static magnetic field. The sample was also oriented horizontally in the microwave cavity, with the static magnetic field parallel to the crystal *ab* plane and perpendicular to the crystallographic *c* axis. The temperature-dependent EPR data were obtained at 9.27 GHz with 100 kHz modulation. Data were collected using a US EPR (Clarksville, MD) SPEX300 data acquisition program.

Transport measurements

Temperature dependent (4–298 K) resistivity measurements were made using a four-probe low-frequency ac technique. Four gold contacts (~3000 Å thick) in a linear arrangement were deposited on a single plate-like crystal (2.5 × 0.9 × 0.2 mm³) of (BEDO-TTF)₄[C₄N₆]₄·H₂O by thermal evaporation, and narrow gauge (0.0127 mm diameter) gold wires were affixed to the contacts using fast-drying silver paint. The sample was fastened on to a chip-holder which attaches to a home-built low temperature dipstick operating from 4.2 to 300 K. A typical run was done by first cooling the sample to the lowest temperature and collecting data while warming. Temperature stability obtained in this set-up has been determined to be ±0.5 K or better over the temperature range measured. Lower temperatures were achieved by using a home-made dilution refrigerator.

Tunnel diode oscillator (TDO) measurements

The electromagnetic response of **3** was investigated by means of a simple inductor-capacitor (LC) tank circuit whose response was driven by a tunnel diode. These types of simple circuits are often used to search for superconducting transitions.^{13,14} Briefly stated, the change in the frequency, *f*, of the oscillator may be approximated by eqn. (1),

$$\frac{\Delta f}{f_0} = G \Delta \lambda \quad (1)$$

where Δ*f* = *f*(*T*_{min}) – *f*(*T*), *f*₀ is the resonant frequency which is nominally 2 MHz in this case, and *G* represents sample geometry factors which are temperature independent.¹⁴ The temperature dependent response is embedded in Δλ, which is the change in skin depth of a metal, or penetration depth in the case of a superconductor.

Results and Discussion

Synthesis and structure of (BEDO-TTF)₄[C₄N₆]₄·H₂O **3**

The title compound was precipitated from a constant-current electrocrystallization cell using a low concentration solution of Na₂C₄N₆·H₂O and 15-crown-5 in a 15% EtOH–methylene chloride solvent mixture. (BEDO-TTF)₄[C₄N₆]₄·H₂O forms as elongated plates which are shiny and black. The X-ray structure was determined at 173 K, and crystallographic data are presented in Table 1. Fig. 1 shows a packing diagram of **3** perpendicular to the long axis of the BEDO-TTF molecules. The unit cell consists of four equivalent BEDO-TTF^{1/2+} cations, one *N,N',N''*-tricyanoguanidinate dianion, and one water solvent molecule. BEDO-TTF molecules align side-by-side to form a 2D array within the *ab* plane as shown in Fig. 2 and 3. As is typical for BEDO-TTF cation-radical salts, the sheets of BEDO-TTF cations are separated by sheets of the counterion.

The *N,N',N''*-tricyanoguanidinate dianions, **2**, form sheets parallel to the *ab* plane that separate the donor layers. The anion sheets accommodate one water solvent molecule per dianion and the water molecules are disordered. The tricyanoguanidinate dianions form dimers through hydrogen bonding with two water molecules as shown in Fig. 4. Each water molecule makes two hydrogen bonds, one to a terminal nitrogen atom on one dianion and one to a central nitrogen atom on the other dianion. The dimers pack in the *ab* plane forming an infinite sheet. In their original description, Subrayan *et al.* point out that **2** is planar with a propeller-like shape.¹¹ In **3**, the central CN₃ unit is planar with all three N–C–N angles adding up to 360°; however, the outer portion of each leg of the propeller is slightly out of the plane. This deviation causes each dianion to be puckered, and within a dimer unit one dianion is puckered upward and the other downward.

Table 1 Crystallographic data and structure refinement for (BEDO-TTF)₄[C₄N₆]²⁻·H₂O

empirical formula	C ₄₄ H ₃₄ N ₆ O ₁₇ S ₁₆
formula weight	1431.73
T/K	173(2)
wavelength/Å	0.71073
crystal system	triclinic
space group	<i>P</i> $\bar{1}$
unit cell dimensions	<i>a</i> = 11.9628(2) Å α = 81.268(1)° <i>b</i> = 14.1016(2) Å β = 70.206(1)° <i>c</i> = 17.0830(3) Å γ = 77.038(1)°
<i>V</i> /Å ³ ; <i>Z</i>	2633.39(7), 2
<i>D_c</i> /Mgm ⁻³	1.806
absorption coefficient/mm ⁻¹	0.737
<i>F</i> (000)	464
crystal size/mm ³	0.34 × 0.30 × 0.04
θ range for data collection (°)	1.27–25.00
limiting indices	−15 ≤ <i>h</i> ≤ 14, −18 ≤ <i>k</i> ≤ 7, −22 ≤ <i>l</i> ≤ 22
reflections collected	16658
independent reflections	8946 [<i>R</i> _(int) = 0.0396]
absorption correction	empirical
min., max. transmission	0.703, 0.977
refinement method	Full-matrix least-squares on <i>F</i> ²
data/restraints/parameters	8913/0/774
goodness-of-fit on <i>F</i> ²	1.019
Final <i>R</i> indices [<i>I</i> > 2σ(<i>I</i>)]	<i>R</i> ₁ = 0.0461, <i>wR</i> ₂ = 0.1012 [5824]
<i>R</i> indices (all data)	<i>R</i> ₁ = 0.0802, <i>wR</i> ₂ = 0.1486
extinction coefficient	0.0021(2)
largest diff. peak and hole/e Å ⁻³	0.718 and −0.414

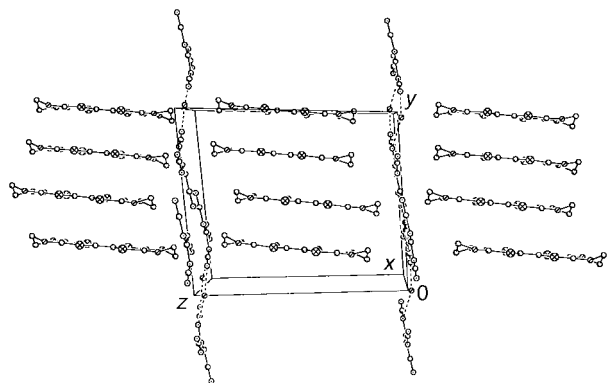


Fig. 1 The packing diagram for **3** including both anions and cations. There are sheets of BEDO-TTF cations separated by layers of *N,N',N''*-tricyanoguanidinate dianions. Hydrogen atoms are omitted for clarity.

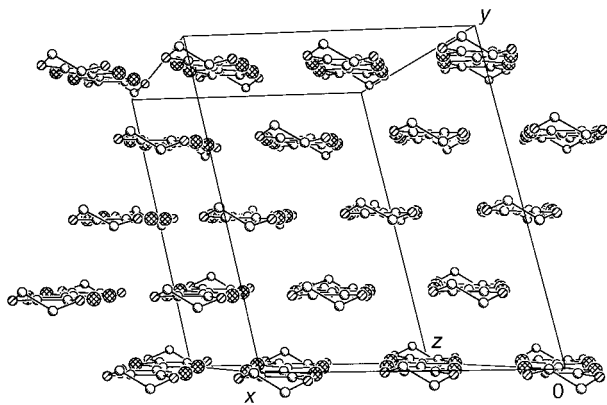


Fig. 2 View of the BEDO-TTF cation layer looking down the long axis of the donor molecule. Numerous S...S, S...O and C-H...O intermolecular contacts exist between molecules within the donor ion sheet, giving the material two-dimensional electronic character. The donor ion packing is the same as the 'I₃' motif characterized by Horiuchi.

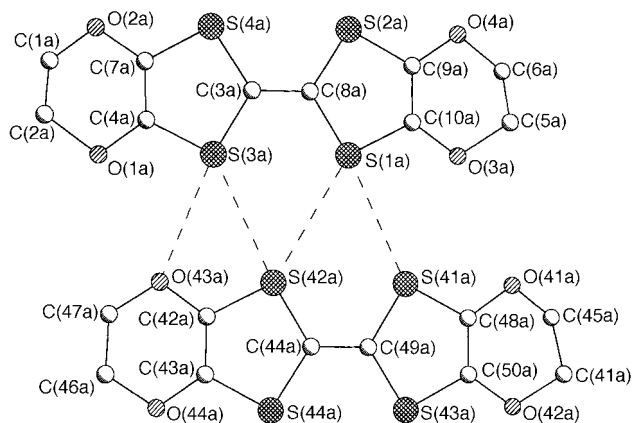


Fig. 3 A side-by-side arrangement of two BEDO-TTF donor molecules. Hydrogen atoms are omitted for clarity. Three short S...S contacts and one S...O contact exist between two molecules. The intermolecular contact distances are S(3a)–S(42a) 3.315, S(1a)–S(42a) 3.486, S(1a)–S(41a) 3.362 and S(3a)–O(43a) 3.218 Å.

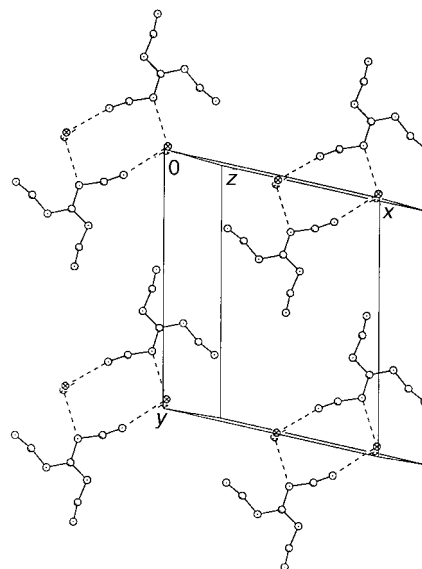


Fig. 4 View of the *N,N',N''*-tricyanoguanidinate dianion layer. The C₄N₆²⁻ anions are puckered with a triskelion shape. Dimers of the C₄N₆²⁻ dianions form through hydrogen bonding with two lattice water molecules (the H₂O molecules are disordered and two positions are shown for each). The dimers pack in the *ab* plane resulting in an infinite two-dimensional layer. (Key for the atoms: crossed circles = oxygen; dotted circles = nitrogen; open circles = carbon.)

This effect occurs in order to accommodate the hydrogen bonds between the dianions and the two water molecules. In addition there are numerous donor–anion interactions present in **3** via ethylene hydrogen atoms on the BEDO-TTF cations and the nitrile groups on the anions which contribute to the puckering of the dianions.

Of the two previously described cation-radical salts with cyano-based dianions, the title compound is isostructural with (BEDO-TTF)₄(HCTMM)·2CH₂ClCHCl₂.¹⁰ The mode of cation packing in **3** is commonly seen in BEDO-TTF cation-radical salts and has been designated the 'I₃' motif by Horiuchi *et al.* after the prototype (BEDO-TTF)₂·I₃.^{6,10} Band structure calculations by Kahlich *et al.*¹⁵ on (BEDO-TTF)₂ReO₄·H₂O, another salt with the 'I₃' motif, have shown that this packing motif gives rise to a two-dimensional Fermi surface. The other cyano-based dianion salt (BEDO-TTF)₄(HCP)·2C₆H₅CN is also metallic but forms with a different packing motif, designated HCP by Horiuchi.¹⁰

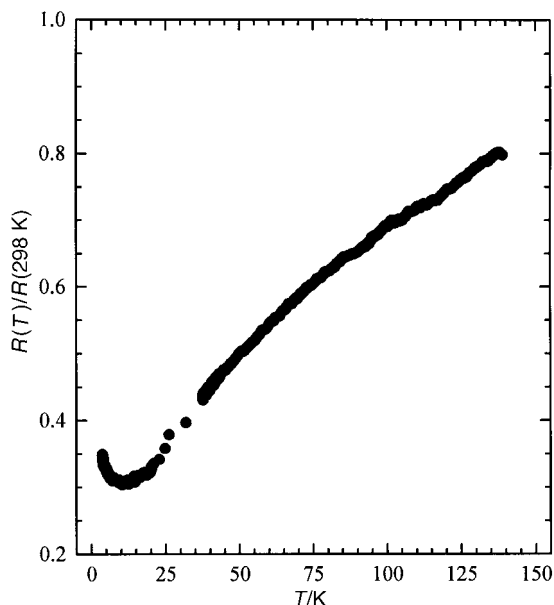


Fig. 5 The temperature dependence of the resistance for a single crystal of **3** normalized by its room temperature value $3 (\pm 1) \Omega$. There is a metal–semiconductor transition at 8 K due to gradual localization of the conduction electrons.

Transport and magnetic properties of $(\text{BEDO-TTF})_4[\text{C}_4\text{N}_6] \cdot \text{H}_2\text{O}$

The organic donor BEDO–TTF has a strong tendency to form donor–acceptor complexes and cation-radical salts which exhibit metallic conductivity down to low temperatures ($< 20 \text{ K}$).^{16,17} This tendency to form ‘metals’ is ascribed to the strong intermolecular interactions normally seen in BEDO–TTF donor layers that gives rise to wide conduction bands. Although BEDO–TTF salts are frequently conductors, the large bandwidths have led to few examples of superconductivity.^{7,9}

Conductivity data for **3** are shown in Fig. 5. $(\text{BEDO-TTF})_4[\text{C}_4\text{N}_6] \cdot \text{H}_2\text{O}$ is metallic at room temperature with $\sigma_{298\text{K}} = 11.5 \text{ S cm}^{-1}$. As the temperature is decreased, the complex remains metallic down to 8 K ($\sigma_{8\text{K}} = 38.5 \text{ S cm}^{-1}$) where an upturn in resistivity occurs indicating the occurrence of a metal–semiconductor transition. Resistivity data taken down to 100 mK show the semiconducting behavior persists with no evidence of a superconducting transition. Low temperature metal–semiconductor transitions have been seen in numerous other BEDO–TTF cation-radical salts.¹⁰ In the case of **3**, the metal–semiconductor transition appears to be due to a localization of the conduction electrons.

Fig. 6 shows the temperature dependence of the electromagnetic response of **3** while using the tunnel diode oscillator (TDO) technique. Near $8.5 (\pm 1) \text{ K}$, the response shows the onset of a change in the signal. While a similar response is expected for a metal–superconductor transition, the resistivity data plotted in Fig. 5 show an increase in resistivity in the same temperature regime. Therefore, the TDO response is signaling an increase in skin depth accompanying the increased resistivity of the sample as the temperature is lowered through the metal–semiconductor transition.

EPR data were obtained with a single crystal of **3** from 4 to 298 K. The EPR lineshape is Lorentzian at all temperatures, becoming Dysonian¹⁸ below 100 K. The characteristic feature of the Dysonian lineshape is the asymmetry of the resonance (Fig. 7) due to skin depth effects.¹⁹ All EPR spectra have been fit to a linear combination of Lorentzian absorption and dispersion assuming a flat-plate geometry using the methods outlined by Chapman *et al.* for magnetic resonance in metallic species.²⁰

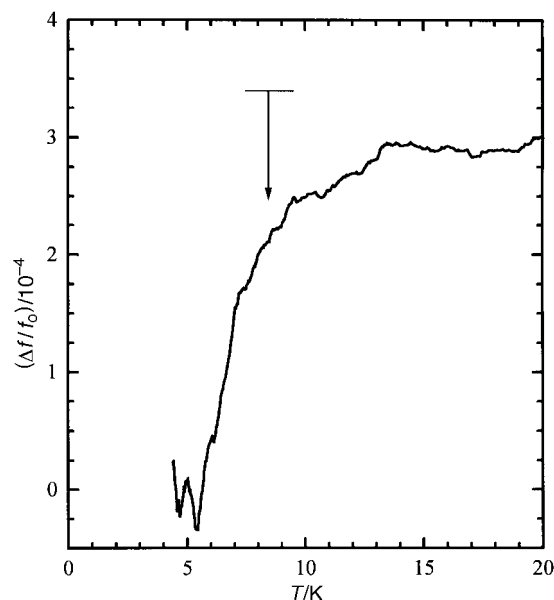


Fig. 6 The temperature dependence of the electromagnetic response of **3** while using the tunnel diode oscillator technique [see eqn. (1)]. The signal is consistent with **3** experiencing a transition from a state with a large skin depth (*i.e.* a poor conductor) at low temperatures to one with a smaller skin depth (*i.e.* a better conductor) at higher temperatures. The arrow indicates the $8.5 (\pm 1) \text{ K}$ metal–semiconductor transition temperature.

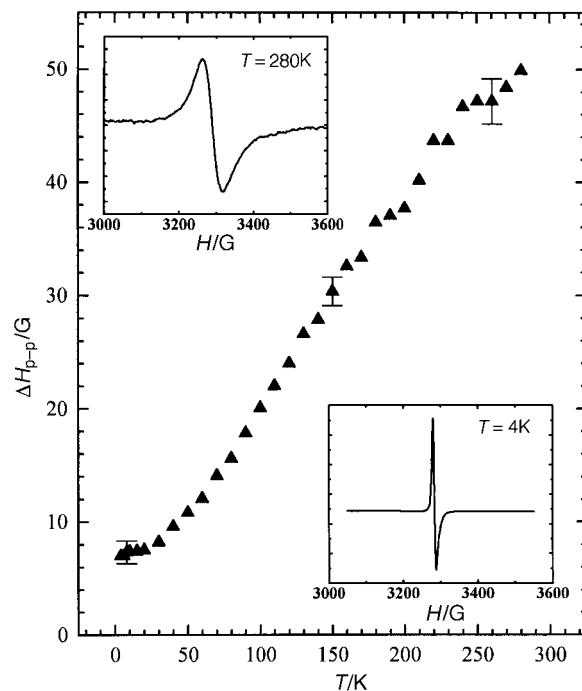


Fig. 7 The temperature dependence of the peak-to-peak linewidth for **3** obtained from the absorption component of the EPR spectra. Representative EPR spectra of **3** at 280 and 4 K, showing the increasing Dysonian character of the resonance as the temperature is lowered, are shown in the insets.

Fig. 7 plots the temperature dependence of the EPR linewidth (ΔH_{p-p}) from 4 to 298 K, with the static magnetic field perpendicular to the *ab* plane of the crystal (*i.e.* the crystal face), determined from the absorption portion of the spectra, with typical spectra at 280 and 4 K shown as insets. $(\text{BEDO-TTF})_4[\text{C}_4\text{N}_6] \cdot \text{H}_2\text{O}$ exhibits a nearly linear decrease in linewidth from 52.2 G at 298 K to 7.8 G at 4 K. This decrease in linewidth as the temperature is lowered is a common feature of organic metals due to reduced electron–

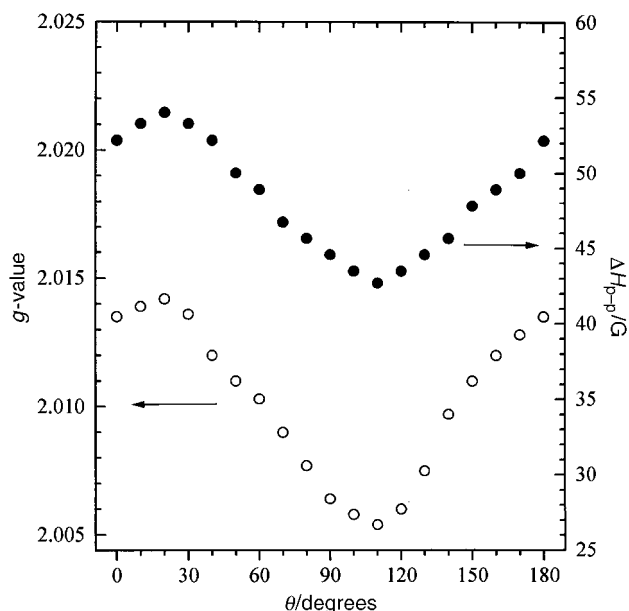


Fig. 8 The angular dependence of (○) the g value and (●) the peak-to-peak linewidth, ΔH_{p-p} , at 298 K for **3**. The directions of the static magnetic field at 0° and 90° are perpendicular and parallel, respectively, to the crystal face (*i.e.* the ab plane).

phonon scattering.^{21–25} The integrated area under the EPR signal for **3** was measured from 4 to 298 K in the same orientation.²⁶ The integrated area,²⁶ obtained from the absorption portion of the measured signal and subsequently corrected for the reduced microwave penetration depth of the sample, is approximately temperature independent down to ~ 50 K where an upturn occurs. The relatively constant integrated area between room temperature and 50 K is consistent with Pauli paramagnetism observed in metallic species. The integrated area data below 8 K can be fit to a Curie law; however, the upturn between 50 and 8 K is not Curie-like. In this temperature regime the increase in the integrated area may be a sign of localization of the conduction electrons.

The g value for **3** is nearly independent of temperature, increasing only slightly from 2.011(1) at room temperature to 2.014(1) at 4 K. The angular dependence of the g value and linewidth were studied at room temperature on a single crystal and the data are plotted in Fig. 8. In this plot, 0° corresponds to the crystal face (ab plane) perpendicular to the static magnetic field while 90° corresponds to the crystal face parallel to the static magnetic field. For both the linewidth and g value, one maximum and one minimum are seen near 20° and 110° , respectively, which are slightly shifted from the crystallographic axes. A consequence of the low crystal symmetry (*i.e.* space group $P\bar{1}$) is that the principal molecular axes of the BEDO–TTF molecules do not correspond with any of the crystallographic axes. From the crystal structure, the long axis of the BEDO–TTF cation forms angles of 90 , 81.1 and 20.5° with the a , b and c axes, respectively. The maximum near 20° corresponds to the static magnetic field parallel to the BEDO–TTF molecular long axis (the central C=C bond), while the minimum near 110° corresponds to the static magnetic field parallel to the BEDO–TTF short molecular axis. The principal g values and the axes of the g tensor were determined by performing a least-squares fitting²⁷ to eqn. (2),

$$g^2 = \sum_{i,j=1}^n g_{ij}^2 I_i I_j \quad (2)$$

where I_i and I_j are the direction cosines of the principal (x , y or z) axes of the BEDO–TTF molecule. The principal g values are $g_{(xx)} = 2.004(1)$, $g_{(yy)} = 2.000(1)$, $g_{(zz)} = 2.014(1)$ which correspond to the static field parallel to the BEDO–TTF molecular

short axis, perpendicular to the molecular plane, and parallel to the molecular long axis, respectively.

Conclusion

A new metallic BEDO–TTF cation-radical salt with a cyano-rich anion, N,N',N'' -tricyanoguanidinate, (BEDO–TTF)₄[C₄N₆] \cdot H₂O, has been synthesized and characterized, and represents a new material which may be added to the growing list of BEDO–TTF based organic metals. This cation-radical salt incorporating the N,N',N'' -tricyanoguanidinate dianion adopts the 'I₃' packing motif found in other BEDO–TTF cation-radical salts.¹⁰ The BEDO–TTF donor molecule network consists of 2D arrays separated by infinite sheets of N,N',N'' -tricyanoguanidinate dianions which form dimers through hydrogen bonding with the lattice water molecules. The title compound is metallic with a room temperature conductivity of 11.5 S cm^{-1} and has σ_{max} of 38.5 S cm^{-1} at 8 K. Below 8 K the salt undergoes a metal–semiconductor transition. The resistivity was probed down to millikelvin temperatures, but no signs of a superconducting transition were found.

This work was supported in part by the National Science Foundation, Grants DMR-9530453 (D.R.T.) and DMR-9200671 (M.W.M.). K.A.A. wishes to acknowledge the National Science Foundation and the University of Florida for funding of the purchase of the X-ray equipment. Partial support for P.G.R. and D.R.T. from the donors of the Petroleum Research Fund, administered by the ACS, is also acknowledged. The authors thank Dr M. Kurmoo for helpful insights.

References

- 1 K. Bechgaard, K. Carneiro, F. G. Rasmussen, K. Olsen, G. Rindorf, C. S. Jacobsen, H. J. Pederson and J. E. Scott, *J. Am. Chem. Soc.*, 1981, **103**, 2440.
- 2 J. M. Williams, J. R. Ferraro, R. J. Thorn, K. D. Carlson, U. Geiser, H. H. Wang, A. M. Kini and M.-H. Whangbo, *Organic Superconductors*, Prentice Hall, Englewood Cliffs, 1992, p. 400.
- 3 J. M. Williams, A. M. Kini, H. H. Wang, K. D. Carlson, U. Geiser, L. K. Montgomery, G. J. Pyrka, D. M. Watkins, J. M. Kammers, S. J. Boryschuk, A. V. Strieby Crouch, W. K. Kwok, J. E. Schirber, D. L. Overmyer, D. Jung and M.-H. Whangbo, *Inorg. Chem.*, 1990, **29**, 3262.
- 4 T. Suzuki, H. Yamochi, G. Srdanov, K. Hinklemann and F. Wudl, *J. Am. Chem. Soc.*, 1989, **111**, 3108.
- 5 T. Suzuki, H. Yamochi, H. Isotalo, C. Fite, H. Kasmai, K. Liou, G. Srdanov and F. Wudl, *Synth. Met.*, 1991, **41–43**, 2225.
- 6 F. Wudl, H. Yamochi, T. Suzuki, H. Isotalo, C. Fite, H. Kasmai, K. Liou and G. Srdanov, *J. Am. Chem. Soc.*, 1990, **112**, 2461.
- 7 M. A. Beno, H. H. Wang, A. M. Kini, K. D. Carlson, U. Geiser, W. K. Kwok, J. E. Thompson, J. M. Williams, J. Ren and M.-H. Whangbo, *Inorg. Chem.*, 1990, **29**, 1559.
- 8 M. A. Beno, H. H. Wang, K. D. Carlson, A. M. Kini, G. M. Frankensbach, J. R. Ferraro, N. Larson, G. D. McCabe, J. Thompson, C. Purnama, M. Vashon, J. M. Williams, D. Jung and M.-H. Whangbo, *Mol. Cryst. Liq. Cryst.*, 1990, **181**, 145.
- 9 S. Kahlich, D. Schweitzer, I. Heinen, S. E. Lan, B. Nuber, H. J. Keller, K. Winzer and H. W. Helberg, *Solid State Commun.*, 1991, **80**, 191.
- 10 S. Horiuchi, H. Yamochi, G. Saito, K. Sakaguchi and M. Kusunoki, *J. Am. Chem. Soc.*, 1996, **118**, 8604.
- 11 R. P. Subrayan, A. H. Francis, J. W. Kampf and P. G. Rasmussen, *Chem. Mater.*, 1995, **7**, 2213.
- 12 G. M. Sheldrick, SHELXTL5, Siemens Analytical X-ray Instruments Incorporated, Madison, 1995.
- 13 G. W. Crabtree, K. D. Carlson, L. N. Hall, P. T. Copps, H. H. Wang, T. J. Emge, M. A. Beno and J. M. Williams, *Phys. Rev. B*, 1984, **30**, 2958.
- 14 P. J. C. Signore, B. Andracka, M. W. Meisel, S. E. Brown, Z. Fisk, A. L. Giorgi, J. L. Smith, F. Gross-Alltag, E. A. Schuberth and A. A. Menovsky, *Phys. Rev. B*, 1995, **52**, 4446.
- 15 S. Kahlich, D. Schweitzer, C. Rovira, J. A. Paradis, M.-H. Whangbo, I. Heinen, H. J. Keller, B. Nuber, P. Bele, H. Brunner and R. P. Shibaeva, *Z. Phys. B*, 1994, **94**, 39.

- 16 H. Yamochi and S. Horiuchi, *Phosphorous Sulfur Silicon Relat. Elem.*, 1992, **67**, 305.
- 17 H. Yamochi, S. Horiuchi, G. Saito, M. Kusunoki, K. Sakaguchi, T. Kikuchi and S. Sato, *Synth. Met.*, 1993, **55**, 2096.
- 18 F. J. Dyson, *Phys. Rev.*, 1955, **98**, 349.
- 19 R. N. Edmonds, M. R. Harrison and P. P. Edwards, *Ann. Rep. Prog. Chem.*, 1985, **82**, 265.
- 20 A. C. Chapman, P. Rhodes and E. F. W. Seymour, *Proc. Phys. Soc., B*, 1957, **70**, 345.
- 21 E. L. Venturini, L. J. Azevedo, J. E. Schirber, J. M. Williams and H. H. Wang, *Phys. Rev. B*, 1985, **32**, 2819.
- 22 D. R. Talham, M. Kurmoo, P. Day, D. S. Obertelli, I. D. Parker and R. H. Friend, *J. Phys. C: Solid State Phys.*, 1986, **19**, L383.
- 23 N. Kinoshita, M. Tokumoto and H. Anzai, *J. Phys. Soc. Jpn.*, 1990, **59**, 3410.
- 24 M. Oshima, H. Mori, G. Saito and K. Oshima, in *The Physics and Chemistry of Organic Superconductors*, ed. G. Saito and S. Kagoshima, Springer-Verlag, Berlin, 1990, vol. 51, pp. 257–261.
- 25 N. Kinoshita, M. Tokumoto and H. Anzai, *J. Phys. Soc. Jpn.*, 1991, **60**, 2131.
- 26 B. H. Ward, PhD Dissertation, University of Florida, 1997.
- 27 R. S. Drago, *Physical Methods in Chemistry*, W. B. Saunders Co., Philadelphia, 1977.

Paper 7/08481A; Received 24th November, 1997